

## Supporting Information

For

### **Hierarchical Chiral MOFs with the Induced Chirality of AIE Ligands Exhibiting the Non-reciprocal CPL**

Hong-Ru Fu,<sup>a,c</sup> Dan-Dan Ren,<sup>a,b</sup> Kun Zhang,<sup>a,b</sup> Shuang Wang,<sup>a</sup> Xu-Jing Yang,<sup>a</sup> Qing-Rong Ding,<sup>c\*</sup> Ya-Pan Wu<sup>b\*</sup>

<sup>a</sup>College of Chemistry and Chemical Engineering, Luoyang Normal University, Luoyang 471934, P. R. China.

<sup>b</sup>College of Materials and Chemical Engineering, China Three Gorges University, Yichang 443002 China.

<sup>c</sup>State Key Laboratory of Structural Chemistry, Fujian Institute of Research on the Structure of Matter, Chinese Academy of Sciences, Fuzhou, Fujian, 350002, China.

\* Corresponding author E-mails: *qrding@fjirsm.ac.cn*, *wyapan2008@163.com*

## Material Characterization

All the chemicals were purchased commercially and used directly. UV-spectra analysis was carried out on Shimadzu UV-2600 spectrophotometer and Hitachi UH4150 spectrophotometer. Elemental analyses of C, H, and N were measured on a Perkin-Elmer 2400 elemental analyzer. Powder X-ray diffraction (PXRD) were performed on a Rigaku Dmax/2400 X-ray diffractometer operating at 40 kV and 100 mA, using Cu-K $\alpha$  radiation ( $\lambda = 1.5406 \text{ \AA}$ ). Thermogravimetric analysis (TGA) was carried out under nitrogen atmosphere on a Q600 SDY TGA-DTA-DSC thermal analyzer from room temperature to 700 °C with a heating rate of 5 °C/min. Quantum yields were tested on an Edinburgh Instruments FLS-980 spectrometer. Photoluminescence (PL) spectra were measured on a Hitachi F4500 luminescence spectrometer. CD spectra were recorded on a JASCO J-810. CPL spectra were measured on a JASCO CPL-300. The images of polarization are measured by upright fluorescence microscopy with 10 objective lens (Leica DM2500).

## Single-crystal X-ray crystallography

Single crystal X-ray analysis of DCF-15/LCF-15 and DCF-16/LCF-16 were performed on a Rigaku SuperNova detector using Mo K $\alpha$  radiation ( $\lambda = 0.71073 \text{ \AA}$ ) at 100 K. The structure of Cd-CBCD was solved with direct methods and refined by the full matrix least-squares on F<sup>2</sup> with SHELXL and Olex2 software. Anisotropic displacement parameters were applied to all non-hydrogen atoms. The hydrogen atoms were included and generated geometrically. The free solvent molecules in Cd-CBCD were highly disordered, and no satisfactory disorder model could be achieved. Thus, the PLATON/SQUEEZE routine was used to remove their diffraction contributions. CCDC-2265022, 2265023, 2245208 and 2245209 contains the supplementary crystallographic data for this paper. A summary of crystallographic data and structure-refinement parameters is given in Table S1 and S2.

**The synthesis of DCF-15 and LCF-15:** Cd(NO<sub>3</sub>)<sub>2</sub>·4H<sub>2</sub>O (60 mg, 0.20 mmol), D-cam (20 mg, 0.10 mmol), TPPE (25 mg 0.04 mmol), DMF (6 ml), n-Butanol (2 ml) and H<sub>2</sub>O (0.5 ml) were mixed in a 20 ml glass vial by ultrasonic agitation for 10 min and kept at 100 °C for five days. Colorless crystals were obtained with a yield of 70% (based on TPPE). Anal. Calcd (%): C, 57.60; H, 6.28; N, 8.02. Found (%): C, 57.56; H, 6.31; N, 8.04. LCF-15 was prepared by the similar process, only using L-cam to replace D-cam. The yields of DCF-15/LCF-15 were calculated to be 78.3% and 78.9% based on the amounts of TPPE ligands.

**The synthesis of DCF-16 and LCF-16:** Zn(NO<sub>3</sub>)<sub>2</sub>·6H<sub>2</sub>O (56 mg, 0.20 mmol), D-cam (20 mg, 0.10 mmol), TPA (25 mg, 0.1 mmol), DMF (3 ml) and DMSO (1 ml) were mixed in a 20 ml glass vial by ultrasonic agitation for 10 min and kept at 100 °C for three days. Colorless crystals were obtained with a yield of 65% (based on TPA). Anal. Calcd (%): C, 57.60; H, 6.28; N, 8.02. Found (%): C, 57.56; H, 6.31; N, 8.04. LCF-16 was prepared by the similar process, only using L-cam to replace D-cam. The yields of DCF-16/LCF-16 were calculated to be 66.7% and 67.1% based on the amounts of TPA ligands.

## The CD and CPL measurements of DCF-15/LCF-15 and DCF-16/LCF-16

CD spectra was measured on a JASCO J-1500 spectrophotometer. The samples were prepared by using the method for infrared measurement. A mixture of DCF-15/LCF-15 or DCF-16/LCF-16 and KBr (crystal/KBr 1:400, weight ratio, total weight of 100 mg) was finely ground and pressed into a transparent pellet with a diameter of 13 mm. The pellet was directly used for measurement

of CD. The wavelength and bandwidth of the monochromator were set to 280.0 and 1.0 nm, and the time-per-point of each sampling point was 0.5 s.

CPL spectra for all samples were recorded on a JASCO CPL-300 spectrophotometer in the solid state with scanning speed. The basic mode is used. Ex slit width, Em slit width, and accumulations of  $100 \text{ nm min}^{-1}$ , 2000  $\mu\text{m}$ , 2000  $\mu\text{m}$ , and 2, respectively. The excitation wavelength was 360 nm and the DV values were about 0.5 V for DCF-15/LCF-15. As for DCF-16/LCF-16, expect that the excitation wavelength was 280 nm, the others are similar to that of DCF-15/LCF-15.

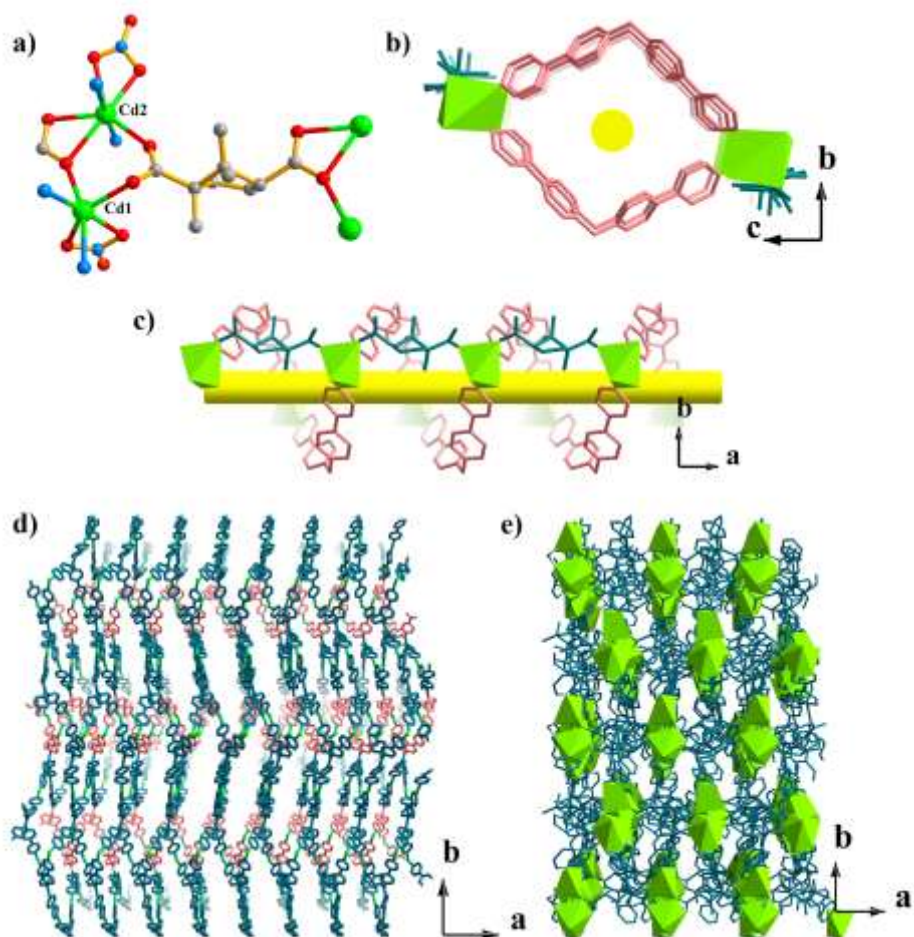


**Figure S1.** (a) The coordination model of D-cam; (b) the left-handed (*M*) helical chain assembled from  $\text{Cd}^{2+}$  ions and TPPE in DCF-15 in the direction of a axis; (c) the left-handed (*M*) helical chain assembled from  $\text{Cd}^{2+}$  ions and TPPE in DCF-15 in the direction of b axis; (d) the left-handed (*M*) helical chain assembled from  $\text{Cd}^{2+}$  ions and TPPE in DCF-15 in the direction of c axis; (e) the 3D structure of DCF-15 in the direction of c axis.

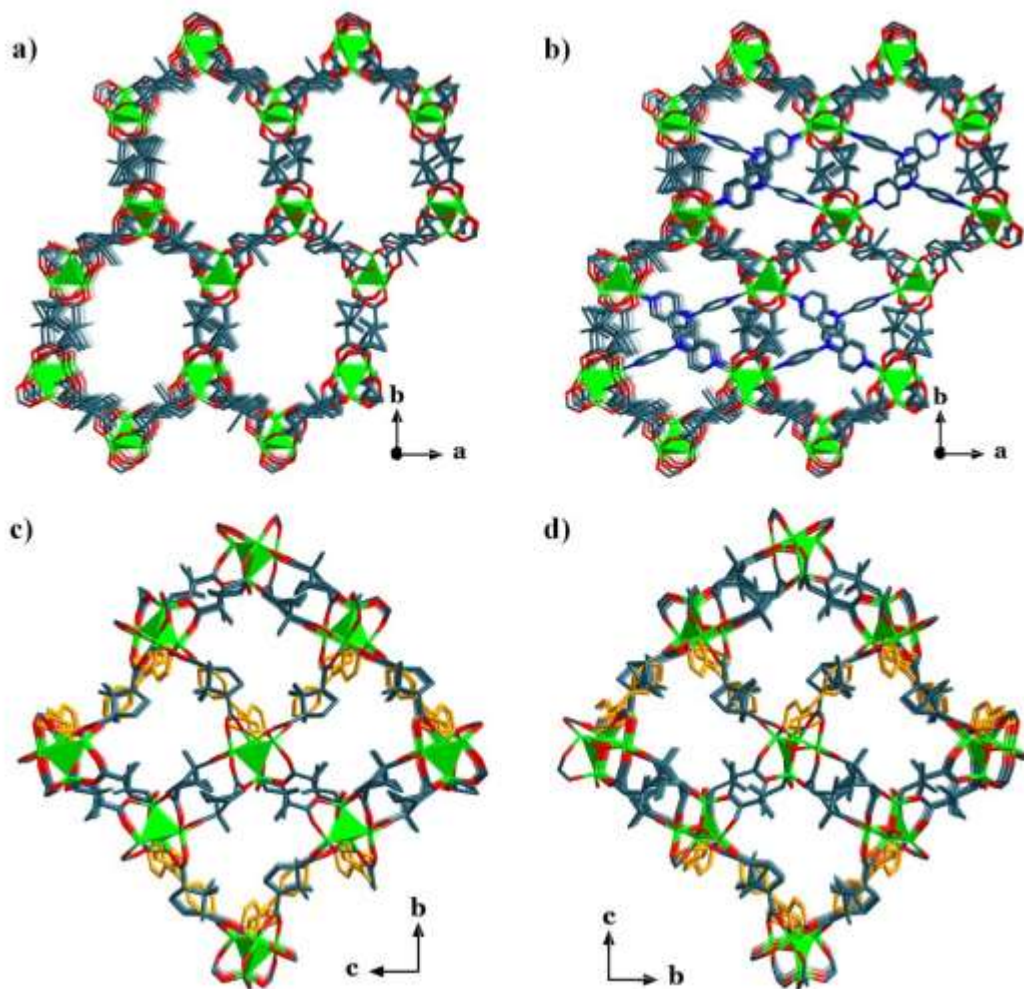


**Figure S2.** (a) The framework assembled of D-cam and  $Zn^{2+}$  ions in DCF-16 in the direction of c axis; (b) the final framework of DCF-16 in the direction of c axis; (c) the final framework of DCF-16 in the direction of a axis; (d) the final framework of LCF-16 in the direction of a axis.

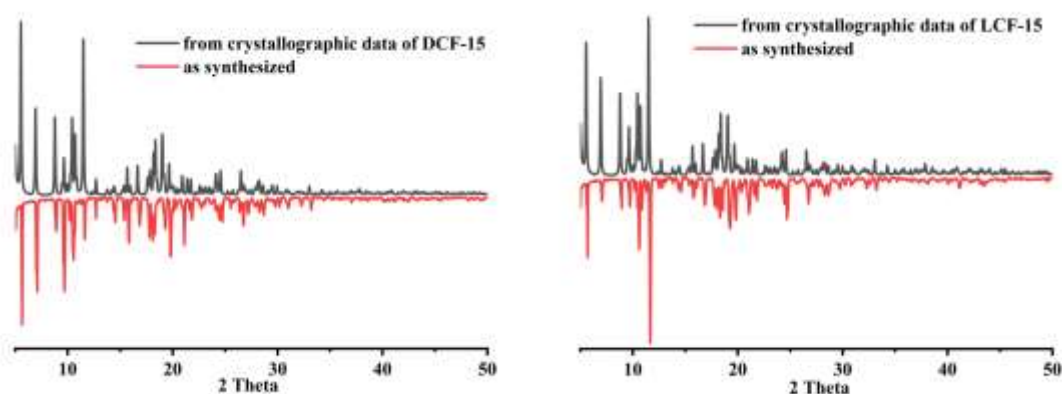


**Figure S3.** PXRD patterns of as-synthesized DCF-15 and LCF-15. All simulated patterns are calculated from the corresponding single-crystal structures. Test conditions: working voltage and current is 40 kV and 40 mA, respectively.

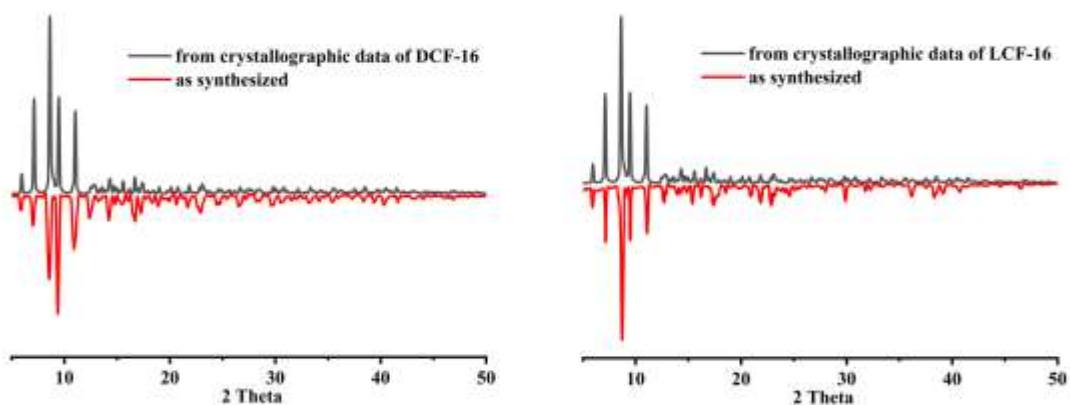


**Figure S4.** PXRD patterns of as-synthesized DCF-16 and LCF-16. All simulated patterns are calculated from the corresponding single-crystal structures. Test conditions: working voltage and current is 40 kV and 40 mA, respectively.

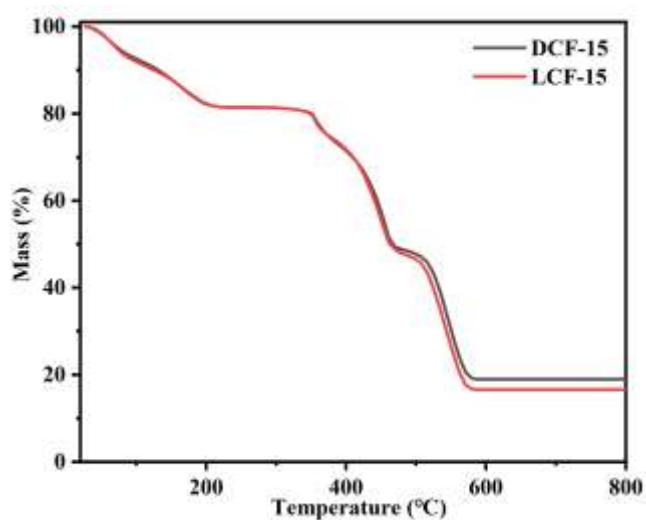


**Figure S5.** TG curves of DCF-15 and LCF-15 under air conditions.

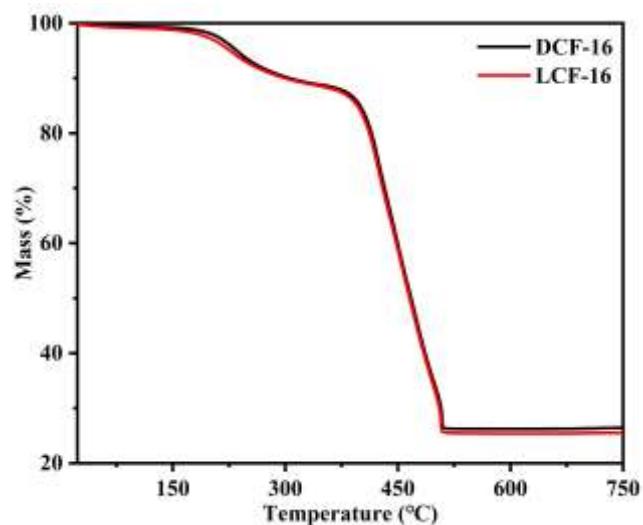


**Figure S6.** TG curves of DCF-16 and LCF-16 under air conditions.

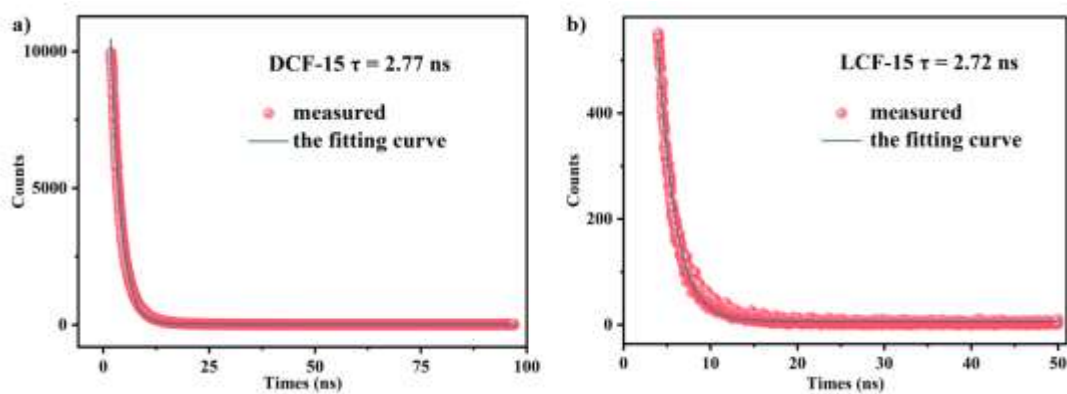


**Figure S7.** The fluorescent lifetimes of DCF-15 and LCF-15 at room conditions.

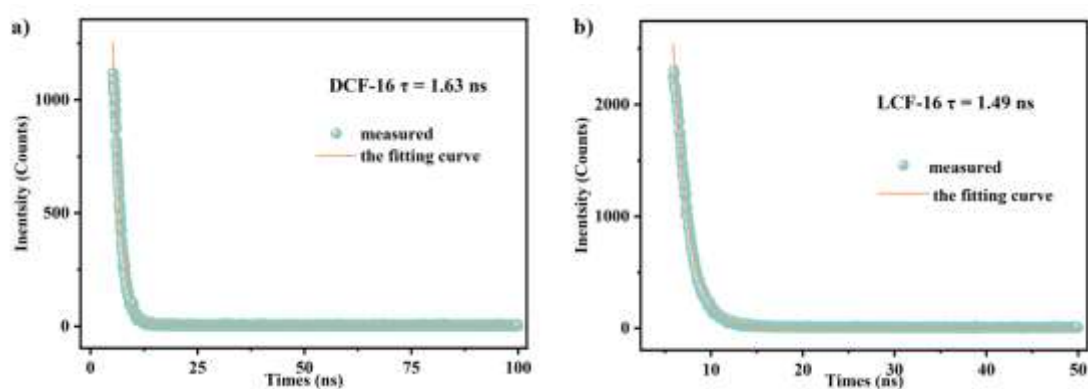


**Figure S8.** The fluorescent lifetimes of DCF-16 and LCF-16 at room conditions.

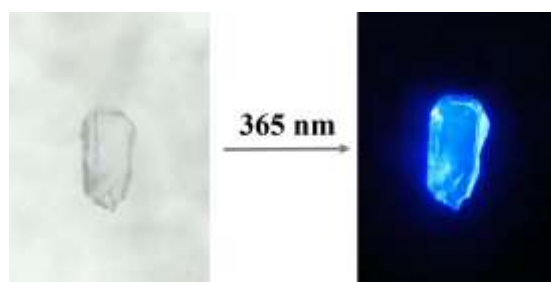


**Figure S9.** The photographs LCF-16 from fluorescence microscope.

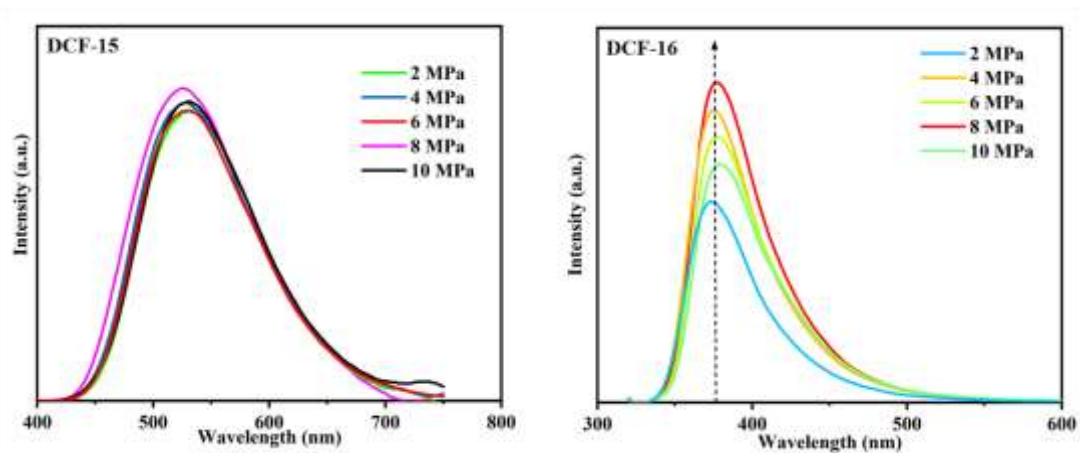


**Figure S10.** The emission behaviors of DCF-15 and DCF-16 under different pressure from 2 to 10 MPa. Using a similar method for the infrared measurement, the samples were prepared by adopting the KBr pellet.

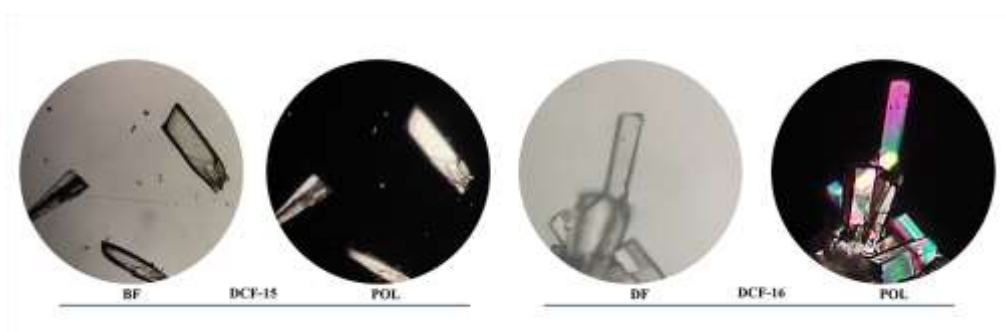


**Figure S11.** The photographs of DCF-15 and DCF-16 were obtained by upright fluorescence microscopy with 10 objective lens (Leica DM2500) under BF (bright field) and POL (polarization) mode, respectively.

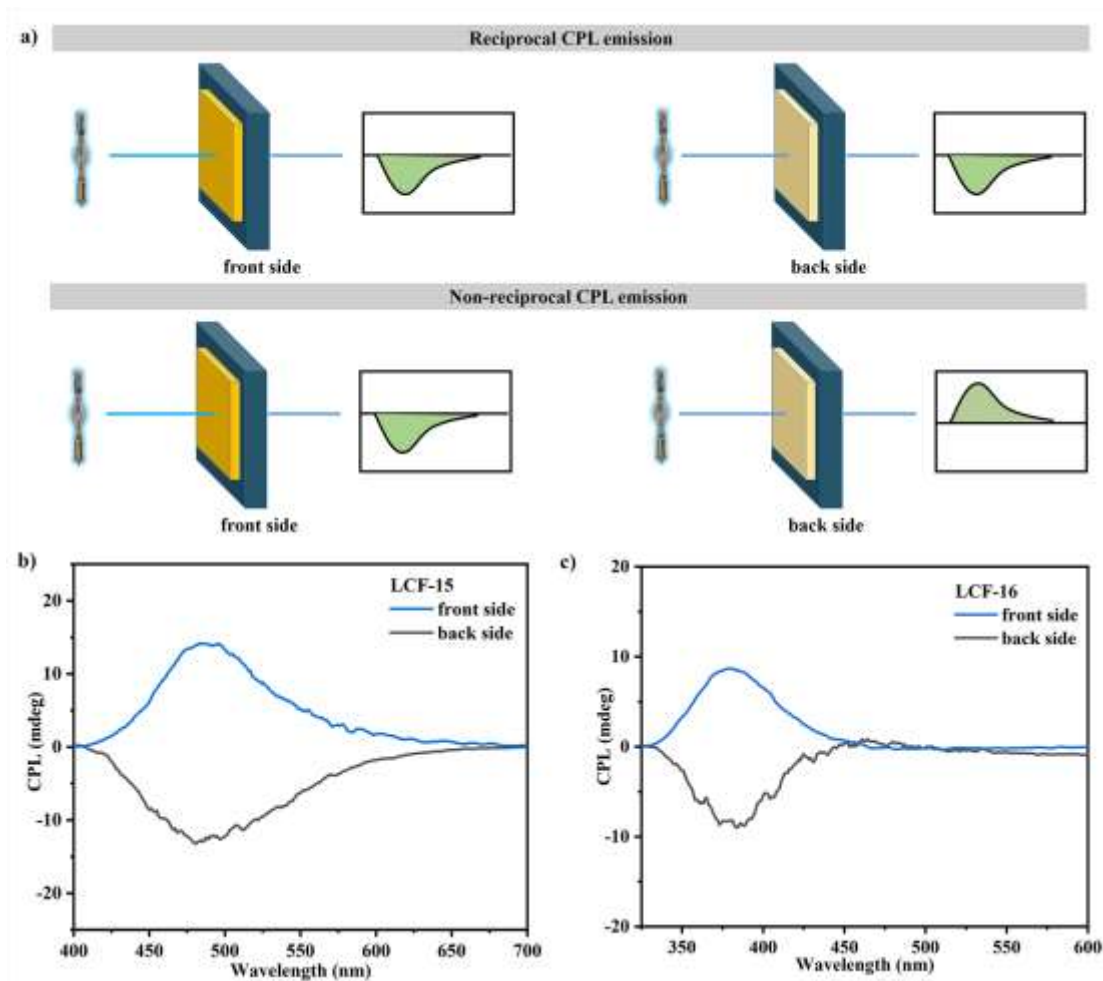


**Figure S12.** (a) Evaluation of reciprocal or non-reciprocal component of CP emission. (b,c) Non-reciprocal CPL of LCF-15 and LCF-16: CPL spectra for the front (blue line) and the back side (red line) of thin film sample.

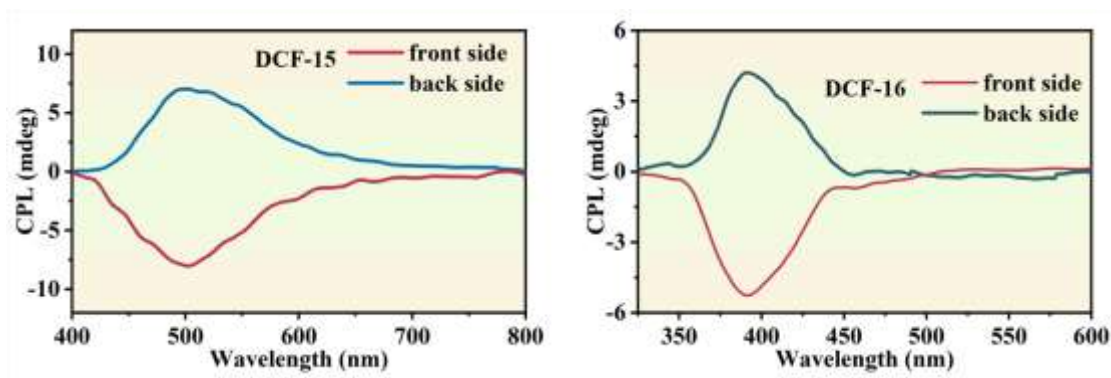


**Figure S13.** Non-reciprocal CPL of DCF-15 and DCF-16: CPL spectra for the front (blue line) and the back side (red line) of thin film sample.

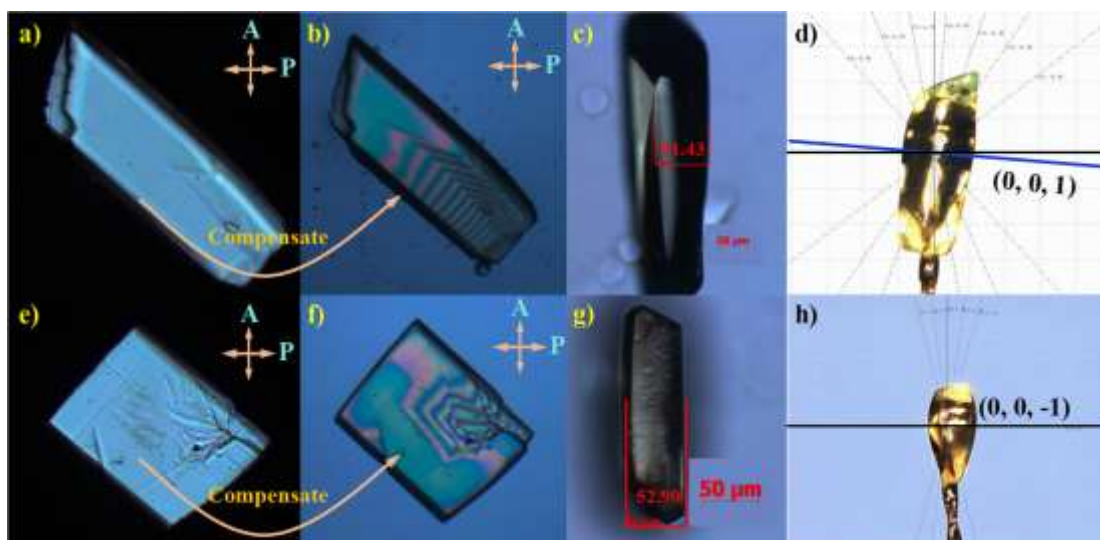


**Figure S14.** The optical properties under a polarizing microscopic, the thickness and the crystallization direction of DCF-15 and LCF-15. (a–d) DCF-15, (e–h) LCF-15.

The birefringence of DCF-15 and LCF-15 were investigated. As shown in Figure S14, in DCF-15 with a (001) crystal plane at a thickness of about 91.43  $\mu\text{m}$ , an optical path difference of 11350.96 nm was obtained, indicating a birefringence of 0.124. Similarly, the (00-1) crystal plane of LCF-15 with the thickness of about 52.90  $\mu\text{m}$  has a birefringence of 0.122.

The optical path difference and thickness were measured on a polarizing microscope (ZEISS Axio Scope. A1) equipped with a compensator.<sup>1</sup> The crystal face indices were ascertained using the single crystal orientation method on the above single crystal diffractometer.<sup>2</sup>

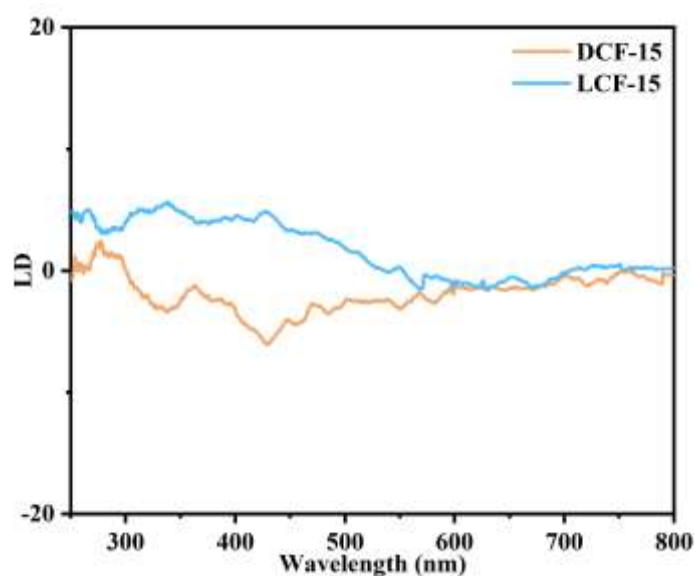


**Figure S15.** LD spectra of DCF-15/LCF-15.

**Table S1.** The crystallographic parameters of DCF-15 and LCF-15

Identification code	DCF-15	LCF-15
Number of CCDC	2245209	2245208
Empirical formula	C <sub>55</sub> H <sub>42</sub> N <sub>6</sub> O <sub>10</sub> Cd <sub>2</sub>	C <sub>56</sub> H <sub>46</sub> N <sub>6</sub> O <sub>10</sub> Cd <sub>2</sub>
Formula weight	1171.74	1187.79
Temperature/K	293	293
Crystal system	orthorhombic	orthorhombic
Space group	<i>P</i> 2 <sub>1</sub> 2 <sub>1</sub> 2 <sub>1</sub>	<i>P</i> 2 <sub>1</sub> 2 <sub>1</sub> 2 <sub>1</sub>
<i>a</i> / Å	9.6554(2)	9.6443(3)
<i>b</i> / Å	17.7129(4)	17.6700(6)
<i>c</i> / Å	36.6589(6)	36.6530(10)
$\alpha$ / °	90	90
$\beta$ / °	90	90
$\gamma$ / °	90	90
Volume/ Å <sup>3</sup>	6269.6(2)	6246.2(3)
<i>Z</i>	4	4
$\rho_{\text{calc}}/\text{cm}^3$	1.241	1.263
$\mu$ / mm <sup>-1</sup>	0.731	0.735
F(000)	2360	2400
Crystal size/ mm <sup>3</sup>	0.10 × 0.20 × 0.30	0.16 × 0.16 × 0.20
Radiation	MoK $\alpha$ ( $\lambda$ = 0.71073)	MoK $\alpha$ ( $\lambda$ = 0.71073)
2 $\theta$ range for data collection/°	6.668 to 58.928	6.646 to 58.504
Index ranges	-8 ≤ <i>h</i> ≤ 13, -21 ≤ <i>k</i> ≤ 22, -48 ≤ <i>l</i> ≤ 32	-13 ≤ <i>h</i> ≤ 10, -17 ≤ <i>k</i> ≤ 23, -24 ≤ <i>l</i> ≤ 49
Reflections collected	22080	20715
Independent reflections	12971 [ <i>R</i> <sub>int</sub> = 0.0411, <i>R</i> <sub>sigma</sub> = 0.0781]	13045 [ <i>R</i> <sub>int</sub> = 0.0385, <i>R</i> <sub>sigma</sub> = 0.0852]
Goodness-of-fit on F <sup>2</sup>	1.041	1.096
Flack	-0.04(2)	-0.050(17)
<i>R</i> <sub>1</sub> [ <i>I</i> > 2 $\sigma$ ( <i>I</i> )]	<i>R</i> <sub>1</sub> = 0.0728, <i>wR</i> <sub>2</sub> = 0.2034	<i>R</i> <sub>1</sub> = 0.0725, <i>wR</i> <sub>2</sub> = 0.2030
<i>wR</i> <sub>2</sub> (all data)	<i>R</i> <sub>1</sub> = 0.0913, <i>wR</i> <sub>2</sub> = 0.2291	<i>R</i> <sub>1</sub> = 0.0912, <i>wR</i> <sub>2</sub> = 0.2237
$R = \frac{\sum   F_o  -  F_c  }{\sum  F_o }, \quad wR = \frac{\{\sum [w( F_o ^2 -  F_c ^2)] / \sum [w( F_o ^4)]\}^{1/2}, \quad w = 1 / [\sigma^2(F_o^2) + (0.1391P)^2 + 0.3555P]$ where $P = (F_o^2 + 2F_c^2) / 3$ for DCF-15.		
$W = 1 / [\sigma^2(F_o^2) + (0.1212P)^2 + 0.7181P]$ where $P = (F_o^2 + 2F_c^2) / 3$ for LCF-15.		

**Table S2. The crystallographic parameters of DCF-16 and LCF-16**

Identification code	DCF-16	LCF-16
Number of CCDC	2265022	2265023
Empirical formula	C <sub>45</sub> H <sub>39</sub> N <sub>4</sub> O <sub>13</sub> Zn <sub>4</sub>	C <sub>45</sub> H <sub>43</sub> N <sub>4</sub> O <sub>13</sub> Zn <sub>4</sub>
Formula weight	1105.36	1100.24
Temperature/K	293	293
Crystal system	orthorhombic	orthorhombic
Space group	<i>P</i> 2 <sub>1</sub> 2 <sub>1</sub> 2 <sub>1</sub>	<i>P</i> 2 <sub>1</sub> 2 <sub>1</sub> 2 <sub>1</sub>
<i>a</i> / Å	13.6565(3)	13.6827(4)
<i>b</i> / Å	14.1762(4)	14.1989(7)
<i>c</i> / Å	29.6834(9)	29.7700(14)
$\alpha$ / °	90	90
$\beta$ / °	90	90
$\gamma$ / °	90	90
Volume/ Å <sup>3</sup>	5746.6(3)	5783.7(4)
<i>Z</i>	4	4
$\rho_{\text{calc}}/\text{cm}^3$	1.263	1.264
$\mu$ / mm <sup>-1</sup>	1.704	1.693
F(000)	2305	2224
Crystal size/ mm <sup>3</sup>	0.12 × 0.13 × 0.17	0.12 × 0.13 × 0.19
Radiation	MoK $\alpha$ ( $\lambda$ = 0.71073)	MoK $\alpha$ ( $\lambda$ = 0.71073)
2 $\theta$ range for data collection/°	6.62 to 58.498	6.752 to 58.380
Index ranges	-11 ≤ <i>h</i> ≤ 18, -38 ≤ <i>k</i> ≤ 19, -19 ≤ <i>l</i> ≤ 12	-11 ≤ <i>h</i> ≤ 18, -19 ≤ <i>k</i> ≤ 12, -38 ≤ <i>l</i> ≤ 40
Reflections collected	19296	22617
Independent reflections	10496 [ <i>R</i> <sub>int</sub> = 0.0296, <i>R</i> <sub>sigma</sub> = 0.0546]	12140 [ <i>R</i> <sub>int</sub> = 0.0344, <i>R</i> <sub>sigma</sub> = 0.0637]
Goodness-of-fit on F <sup>2</sup>	1.027	1.032
Flack	0.017(7)	0.017(8)
<i>R</i> <sub>1</sub> [ <i>I</i> > 2 $\sigma$ ( <i>I</i> )]	<i>R</i> <sub>1</sub> = 0.0532, <i>wR</i> <sub>2</sub> = 0.1473	<i>R</i> <sub>1</sub> = 0.0527, <i>wR</i> <sub>2</sub> = 0.1325
<i>wR</i> <sub>2</sub> (all data)	<i>R</i> <sub>1</sub> = 0.0662, <i>wR</i> <sub>2</sub> = 0.1565	<i>R</i> <sub>1</sub> = 0.0663, <i>wR</i> <sub>2</sub> = 0.1413
$R = \frac{\sum   F_o  -  F_c  }{\sum  F_o }$ , $wR = \frac{\{\sum [w( F_o ^2 -  F_c ^2)^2] / \sum [w( F_o ^4)]\}^{1/2}}$ , $w =$ 1/[ $s^2(F_o^2) + (0.0982P)^2 + 1.9486P$ ] where $P = (F_o^2 + 2F_c^2)/3$ for DCF-16. $w = 1/[s^2(F_o^2) + (0.0766P)^2 + 2.2395P$ ] where $P = (F_o^2 + 2F_c^2)/3$ for LCF-16.		

**REFERENCES**

1. H. Sha, R. Su, Z. Xiong, Z. Wang, P. Shan, C. He, X. Yang, X. Long, Adv. Optical Mater. 2021, 9, 2100080.
2. X. Xu, F. Wang, W. Xu, H. Lu, L. Lv, H. Sha, X. Jiang, S. Wu, S. Wang, Adv. Sci. 2023, 10, 2206833.